

## **Mitigation of Frequency Deviation with Resonant Controller in Microgrid with the Robust Control of an Attached Storage System**

**S. Muqthiar Ali<sup>1</sup>, P.B. Chennaiah<sup>2</sup> and Y. Lakshmi Prasanna<sup>3</sup>**

*<sup>1,2</sup>Assistant Professor (Department of EEE) and <sup>3</sup>PG Student (Department of EEE),*

*<sup>1,2,3</sup> Annamacharya Institute of Technology & Sciences (A.I.T.S),  
Rajampet, Kadapa -516126, Andhra Pradesh, India.*

### **Abstract**

Recent development in the small scale power generation using distributed energy resources combined with application of power electronic systems initiated the researchers to the concepts of future power generation technologies such as micro grid. The paper presented involves the control techniques required for the reduction of microgrid frequency deviations. Mainly these frequency deviations are caused by load disturbances and renewable energy sources as they are associated with it because of their inherent variability. In this proposed work, we consider a microgrid where fossil fuel generators and renewable energy sources are combined with a reasonable sized, fast acting battery-based storage system and we developed a robust control technic for reduction of frequency deviation, with the presence of significant (model) uncertainties. The main advantages of the proposed system work is obtained by comparing system frequency deviation between the proposed system (designed via synthesis) and the reference system which uses governors and conventional PID control to cope with load and res transients. The MATLAB/SIMULINK results by using Resonant model has showed that frequency deviation reduction in microgrid with an attached storage system, where it controls and improves the real power, and frequency.

**Keywords:** Energy storage, microgrid, power systems, and smart grids.

## I. INTRODUCTION

Now a day, fossil fuel is the main energy supplier of the worldwide economy, but the recognition of it as being a major cause of environmental problems makes the mankind to look for alternative resources in power generation. Moreover, the day-by-day increasing demand for energy can create problems for the power distributors, like grid instability and even outages. The necessity of producing more energy combined with the interest in clean technologies yields in an increased development of power distribution systems using renewable energy. Among the renewable energy sources, hydropower and wind energy have the largest utilization nowadays. More and more renewable energy sources are being connected to power systems, often via inverters. The MG concept provides a new level of controllability in smart grid paradigm. The main issues of MG operation are interactions between DG units and the main grid, frequency control and regulation in islanded mode.

Microgrids are essentially modern, small scale (electrical) power distribution systems. They afford numerous benefits, such as enhancing system reliability, reducing capital investment and carbon footprint, and diversifying energy sources. Microgrids contain several generators, whose sizes may range from several tens of kilowatts to a few megawatts.

Renewable energy sources include photovoltaic power, hydro power and wind power. Due to the cost effectiveness of wind turbine generation (WTG), it is one of the fastest growing clean power sources. However, since the output power of WTG is proportional to the cube of the (varying) wind speed, it significantly impacts system stability, and can cause large frequency and voltage ( $F&V$ ) deviations in a microgrid. In this paper we will focus on control of (real) power to reduce frequency deviations.

## II. SYSTEM SETUP AND MODELING

A typical setup of a microgrid with storage system is shown in Fig. 1. The energy sources include both conventional and renewable generation systems. On the common bus-bar are energy sources, variable loads, and also a battery-based storage system. The green blocks indicate that particular component is under control for desired performance. This system can be readily extended into more complex microgrids, with additional generators, loads, bus-bars, transmission lines, and storage systems. The essential idea is to increase the usage of renewable energy, and so reduce the fossil fuel consumption, while at the same time maintaining system stability. Here system stability is reflected by incurring only limited system frequency deviations, despite the presence of significant transients [7].

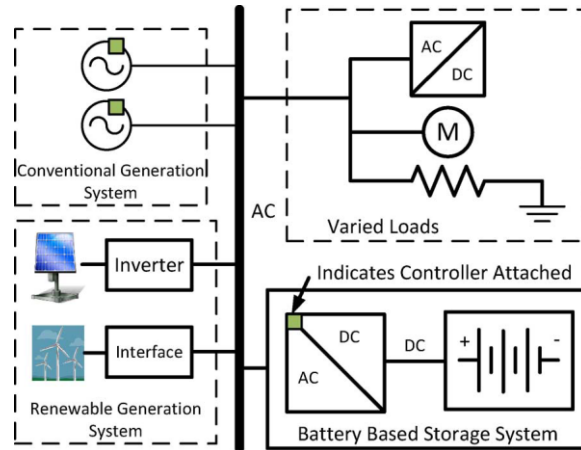


**Figure 1:** Structure of microgrid with attached storage system

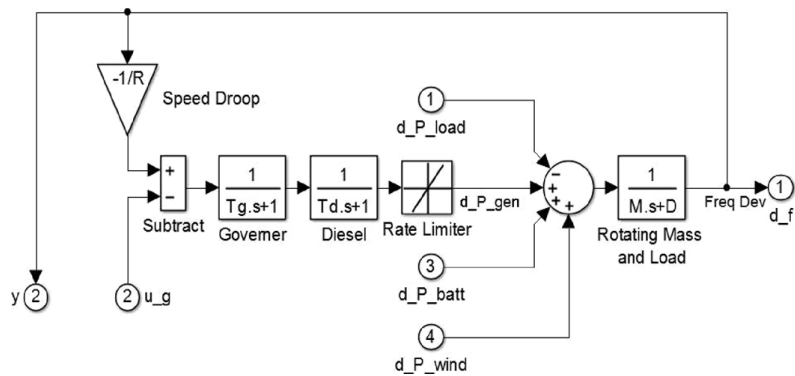


**Figure 2:** Conventional generator (Small Power System)

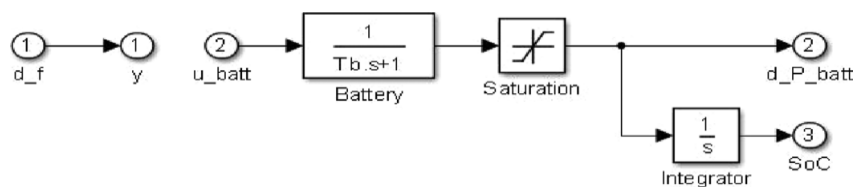


**Figure 3:** Battery model

Low frequency load transients are handled by conventional generators (utilizing diesel or natural gas engines as their prime mover). In order to maintain the nominal frequency in such a system, more advanced control techniques are required to deliver the system performance requirements [8]. In order to minimize the frequency deviation ( $\Delta f$ ), a mathematical model is used for system analysis and controller design. This model consists of three parts: conventional generator (CG), storage system (SS) and Wind Turbine Generator (WTG).

The corresponding Simulink models are shown in Figs. 2–4. However these models still capture the essential power/frequency tradeoffs in such systems. Since  $\Delta f$  is caused by the imbalance between the power generated and the power consumed by the load.

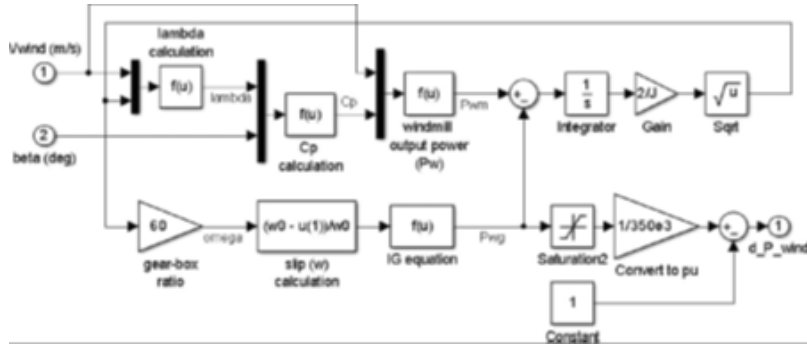


Figure 4: Wind turbine generator model

Hence, the load variation, the SS output variation and WTG output variation are denoted as:  $\Delta P_{Load}$ ,  $\Delta P_{Wind}$ , and  $\Delta P_{batt}$  respectively. These three signals are summed at the summing block in the CG model along with the CG output variation  $\Delta P_{gen}$ .

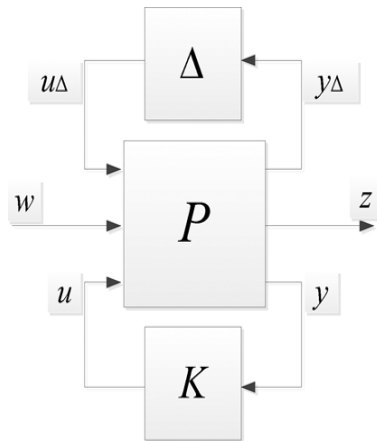
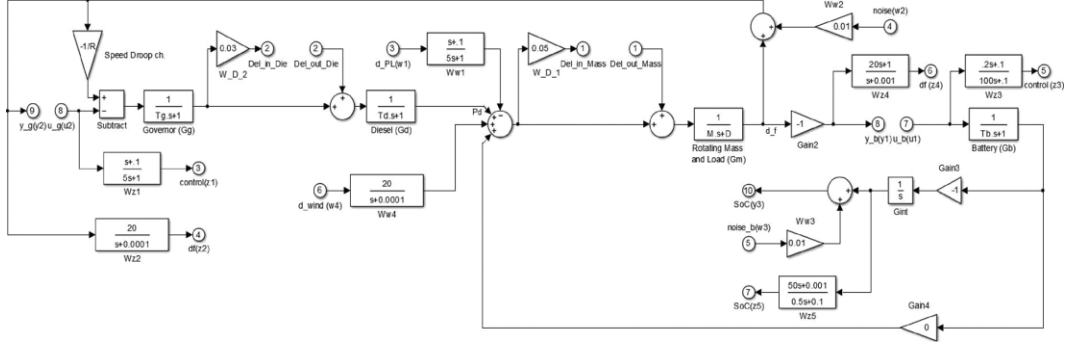


Figure 5: Control configuration for  $\mu$ -synthesis

In our model,  $\Delta P_{batt}$  and  $\Delta P_{gen}$  are controlled power deviations, as shown in Figs. 2 and 3; the control signals are ‘ $u_g$ ’ and ‘ $u_b$ ’ respectively.  $\Delta f$  is considered as the error signal. The controller receives measurements ‘ $y$ ’ and outputs actuation/control signals ‘ $u$ ’. Although  $\Delta P_{batt}$  is a controlled output, the output is limited by a saturation block so as to prevent fast charge and discharge. In addition, the State of Charge (SoC) variation of the SS is modeled by integrating its output power deviation. It is controlled indirectly by commanding  $\Delta P_{batt}$ . Meanwhile,  $\Delta P_{Load}$  and  $\Delta P_{wind}$  are considered as perturbations to the system in the robust controller  $\mu$  synthesis.



**Figure 6:** Plant with model uncertainties for synthesis design.

$P_{wind}$  is “0” unless the angular speed of the gearbox output is higher than the synchronous angular speed. A fixed pitch angle of 10 is used. Our controller does not command the WTG, rather the WTG produces power according to the given wind speed profile (and hence acts as an unknown “disturbance” as far as our system is concerned). Tip speed ratio ( $\lambda$ ), power coefficient ( $C_p$ ), windmill output ( $P_{wm}$ ), Slip ( $S$ ) and WTG output power ( $P_{wg}$ ) as shown in Fig. 4, and are given as:

$$\lambda = R_w \cdot W / V_{wind} \quad (1)$$

$$C_p = f(\lambda, \beta) \quad (2)$$

$$P_{wm} = C_p(\lambda, \beta) V_w^3 \rho A / 2 \quad (3)$$

$$S_s = (\omega_0 - \omega) / \omega_0 \quad (4)$$

$$P_{wg} = -3V^2 S_s(1+S_s) R_2 / (R_2 - S_s R_1)^2 + S_2 (X_1 + X_2)^2 \quad (5)$$

where  $V_{wind}$  is the wind speed,  $A$  is windmill rotor cross section area,  $\omega_0$  is synchronous angular speed, and  $\omega$  is angular rotor speed for a windmill.

These perturbations are usually lumped together in a structured uncertainty description  $\Delta$ , where  $\Delta = \text{diag}(\Delta_i)$  is block diagonal Fig. 5.

$$\mu(M) = \frac{1}{\Delta \min \{|\sigma(\Delta)| \mid \det(I - M\Delta) = 0\}} \quad (6)$$

### III. CONTROLLER DESIGN

We use the D-K iteration approach for  $\mu$ -synthesis controller design. This aims to deliver a closed-loop system with optimized performance in the presence of disturbance signals whilst at the same time retaining robustness to system model uncertainties. In order to precisely specify the robustness and performance criteria, the first step is to decide upon the design system interconnection.

### ***A. Uncertainty in the System***

Nominal models of the small power system and battery are shown in Figs. 2 and 3. Multiplicative model uncertainties of 5% and 3% are added to model blocks ‘Diesel’ and ‘Rotating Mass and Load’ to represent modeling errors as shown in Fig. 6. Unmolded high frequency dynamics can also be included as additional perturbations, but we do not do so here. Measurement noise is added to the frequency deviation and SoC signals.

### ***B. Disturbance Signals on the System***

Two major disturbances in the system arise from variations in load and renewable source (WTG) generation. Note that load draws power from the system, but WTG injects power into the system. In our system, SoC sensor and speed sensor noises are considered.

### ***C. Penalty Signals***

The signals we choose to penalize in the design interconnection effectively specify the performance criteria for the controller design optimization process. In order to minimize the system frequency deviation, the first penalized signal is the output  $\Delta f$ . In order to limit excessive usage of the storage system, its SoC signal is penalized as well

### ***D. Design of $\mu$ -synthesis Controller***

The given Simulink model in Fig. 6 is first linearized with an operating point of 0. As shown in Fig. 6, there are 12 first order transfer functions, which indicates the system has 12 states. The state-space representation (matrices A, B, C, D) of the linearized open-loop plant model (P in Fig. 5) is obtained using the MATLAB™ command ‘linmod’ (applied to Fig. 6), resulting in a system of order 12.

The block-diagonal uncertainty structure  $\Delta$ , as shown in Fig. 5, is then obtained as an uncertain linear time-invariant object. The Linear Fractional Transformation (LFT) of the linearized uncertain plant (P) and the block diagonal uncertainty structure ( $\Delta$ ) is taken to obtain the weighted, uncertain control design interconnection model. We use the DK-iteration algorithm for  $\mu$ -synthesis in Matlab's Robust Control Toolbox to design a  $\mu$ -optimal robust controller K for our uncertain model. The iterative algorithm combines  $H_\infty$ -synthesis and  $\mu$ -analysis to deliver both robustness to uncertainties and optimized performance.

The PID controller is tuned based on the nominal plant. We utilize the Ziegler-Nichols method for PID tuning, and the PID comparison case is implemented with 100% battery attached.

## **IV. SIMULATION AND DISCUSSION**

In this section we show a series of simulation results for the  $\mu$ -synthesis and PID controllers. The load and WTG output deviation in pu ( $\Delta PL$  and  $\Delta PW$ ) are shown in Fig. 7. is about 100% of  $\Delta PL$ .

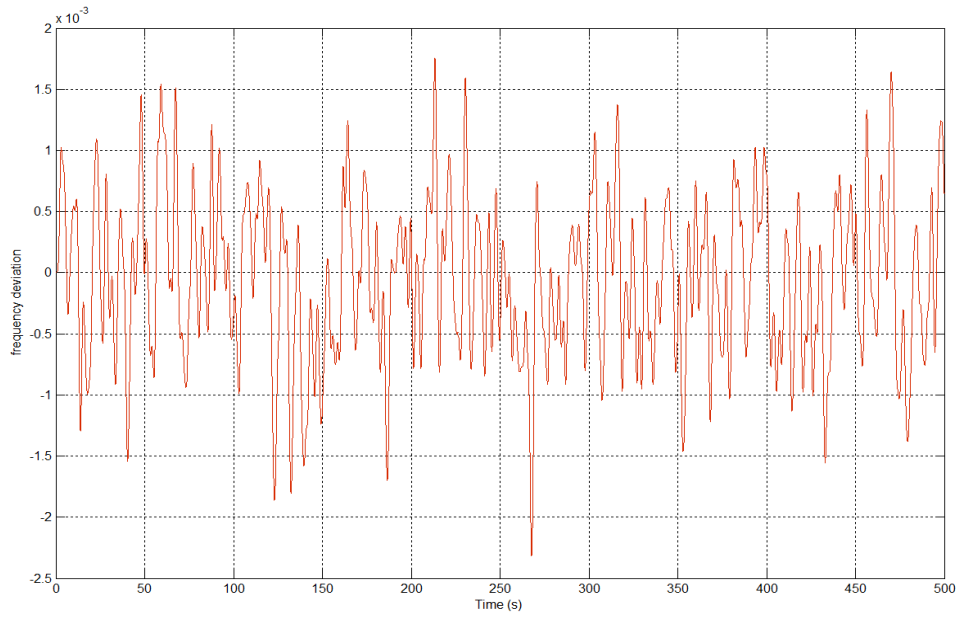


**Figure 7:** Frequency deviation with control and maximum battery power

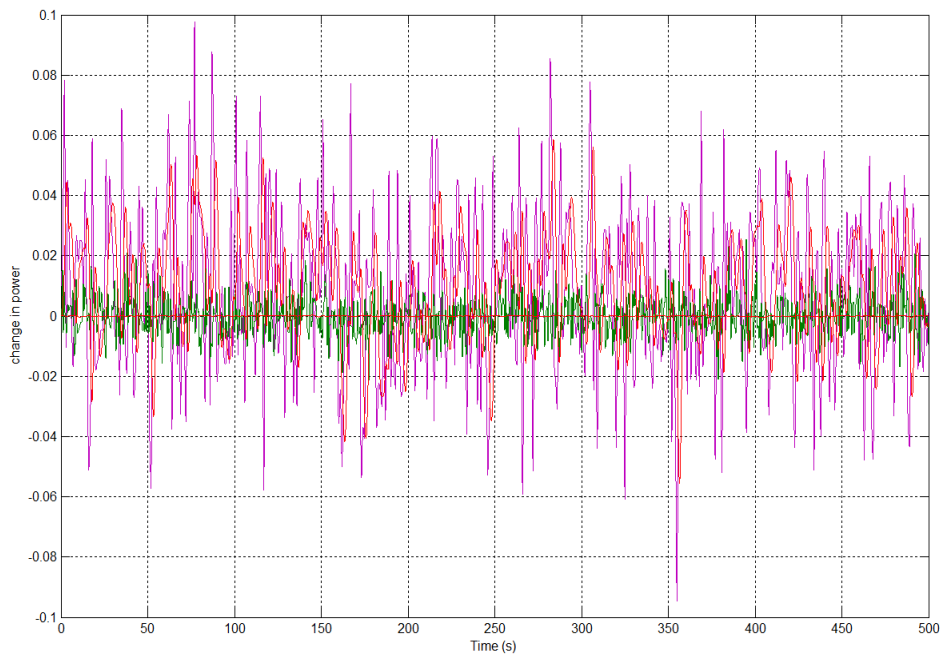


**Figure 8:** Power variations with maximum rated battery power

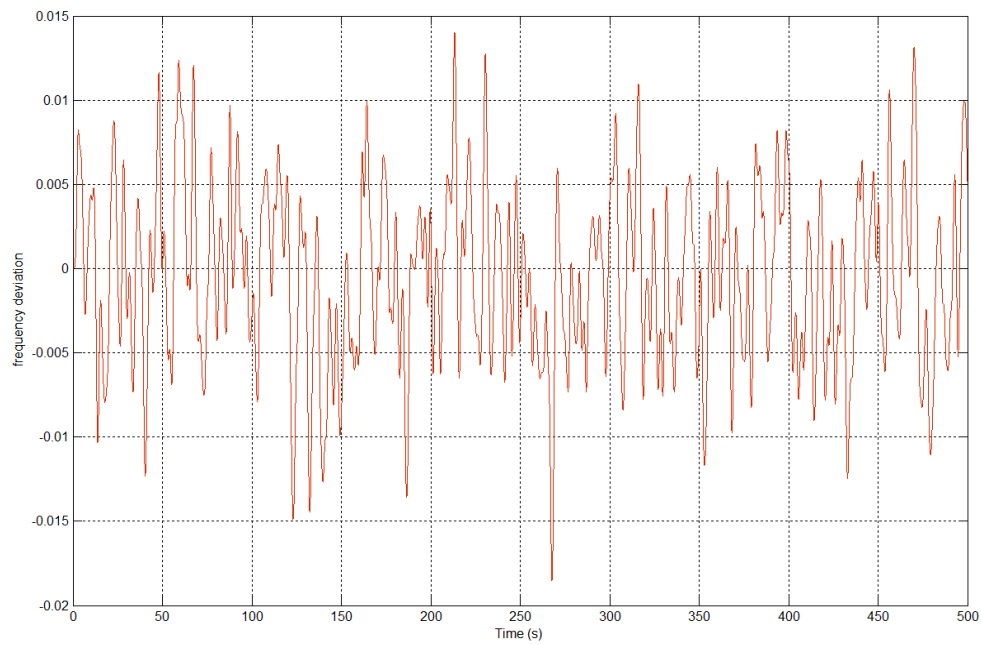


**Figure 9 (a):** Frequency deviation with  $\mu$  control for zero percent battery

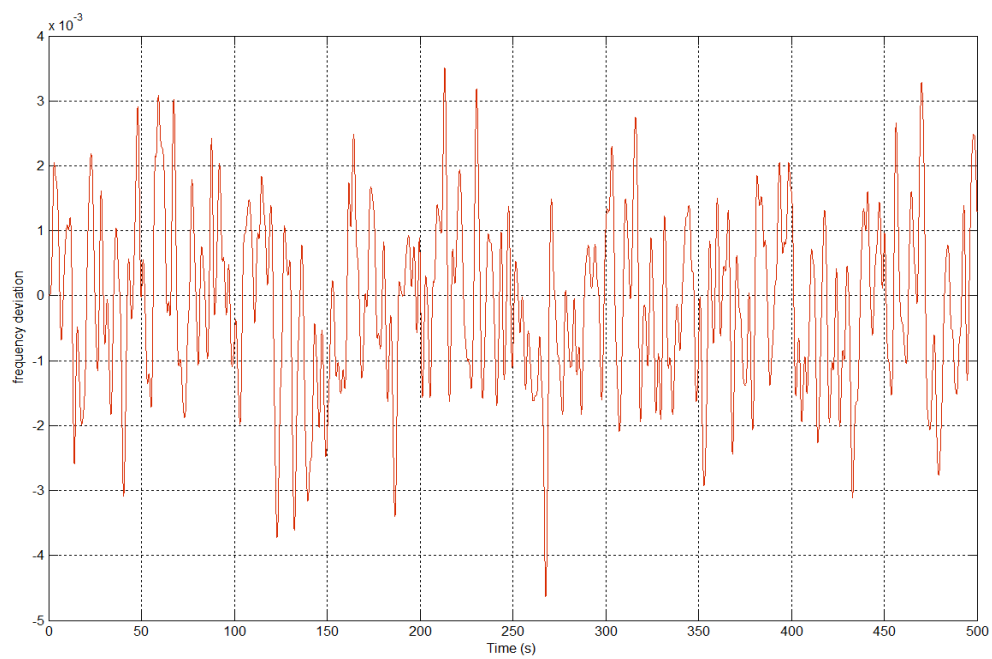


**Figure 9 (b):** Frequency deviation with  $\mu$  control for three percent battery.

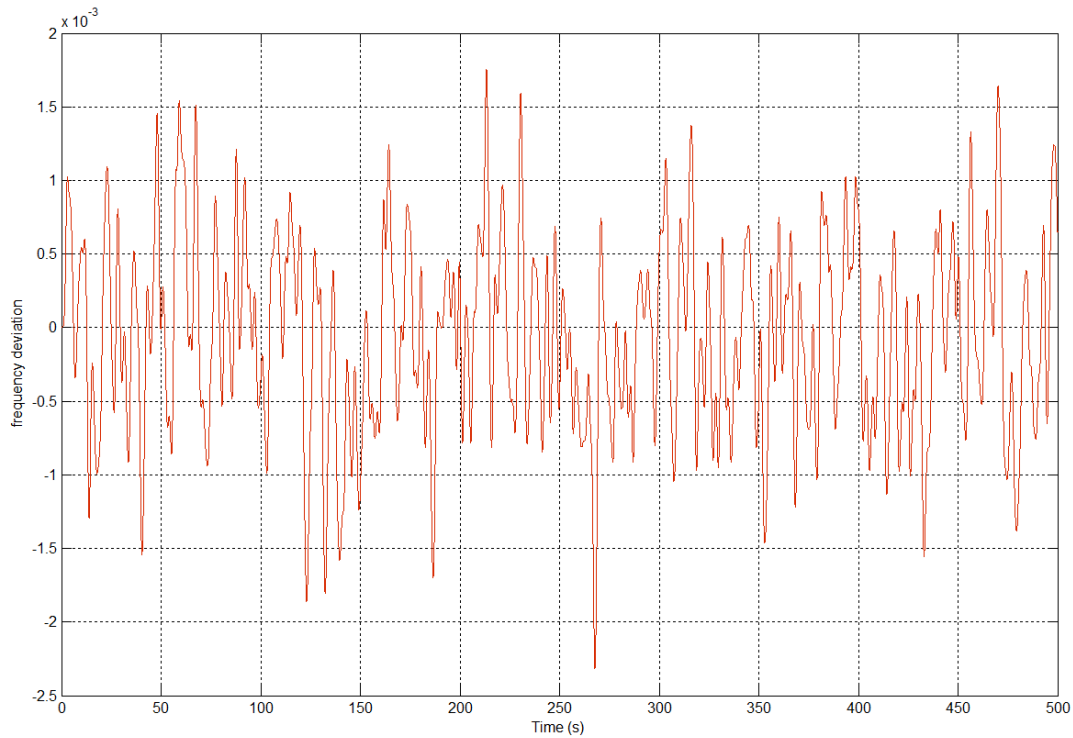


**Figure 9(c):** Frequency deviation with  $\mu$  control for 100 percent battery.

Fig. 7 shows the frequency deviation ( $\Delta f$ ) under  $\mu$  control for 500 s. In this simulation, no constraints were added to the battery, which can deliver its maximum rated power. It can be seen that the peak  $\Delta f$  is about 0.57%, occurring at 307 s. From This causes the system frequency to increases and so  $\Delta f = f_o - f$  will decrease, where  $f_o$  is the nominal frequency.

The load and WTG output variations have steep transients in this time interval, and the load and output power of each power source are compared in Fig. 8, which shows individual generation/load power deviations from the nominal value. For instance, as shown in Fig. 8, at 248 s the generator increases its output power by 7% to match the 5% increase in load and 2% decrease in wind generation. The generator output follows the net load (combined load and WTG) variations and provides the major portion of power. The battery is reacting to the high frequency transients while keeping its SoC around the desired operating point.

At 307 s, load increases by 0.1 p.u and WTG output decreases by 0.02p.u at the very same time. Hence the biggest load transient occurs as shown in Fig.9 shows the frequency variation under control for a variety of different battery scenarios. Fig.10 shows how the power varies for load, generator and wind with no battery system attached.

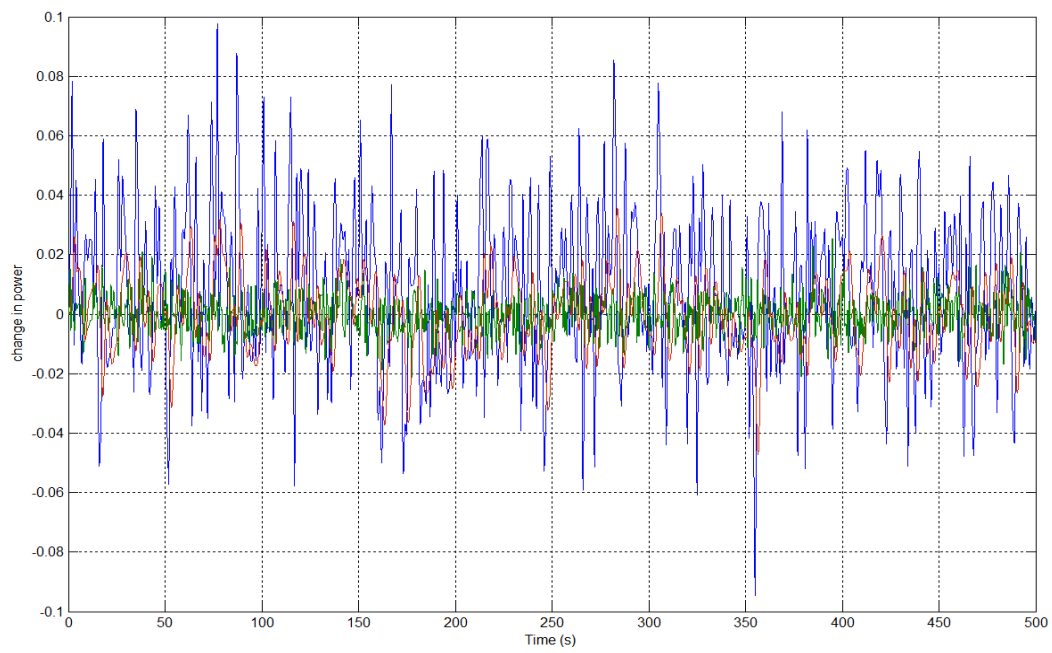


**Figure 10:** Power variation without attached battery

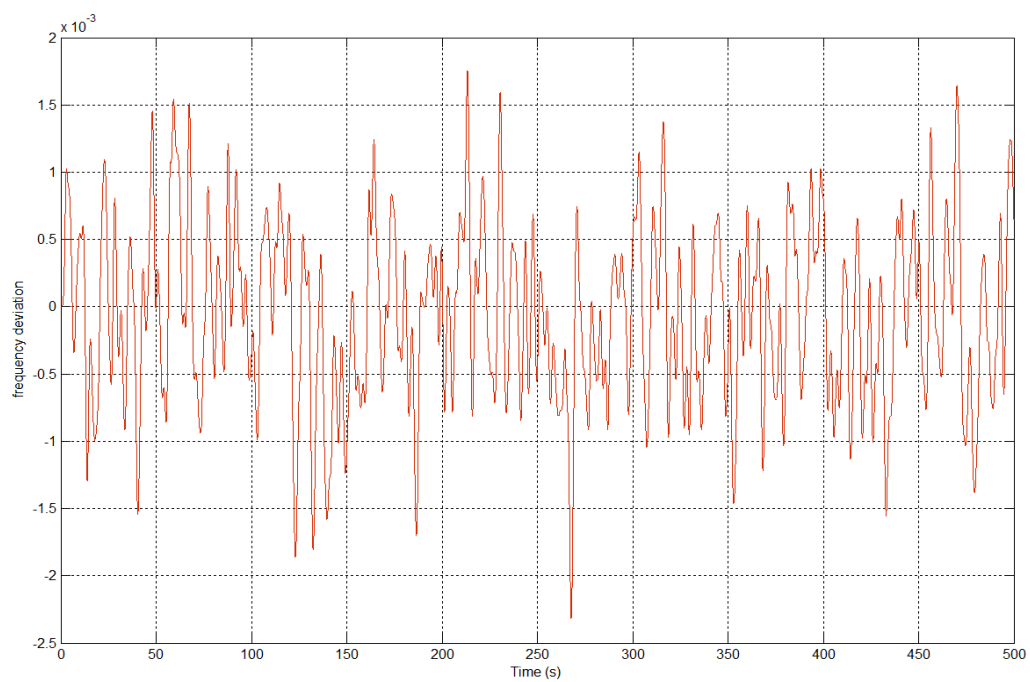


**Figure 11 (a):** Frequency deviations of  $\mu$  synthesis with full battery attached.

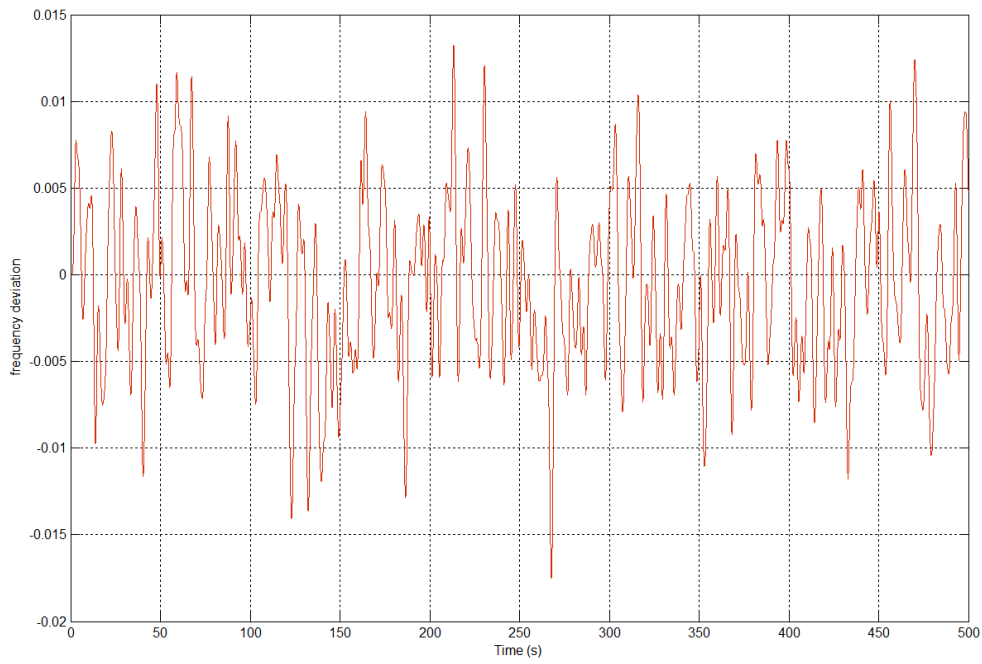


**Figure 11 (b):** Frequency deviations of PID with full battery attached

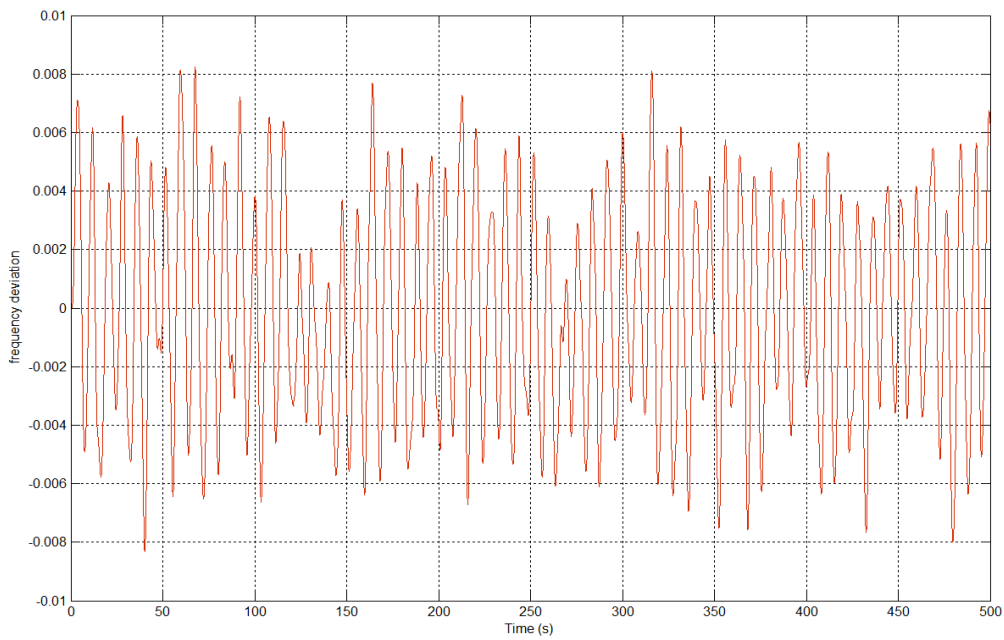


**Figure 12 (a):** Frequency deviation of  $\mu$  synthesis with 10% model uncertainty and measurement noise.

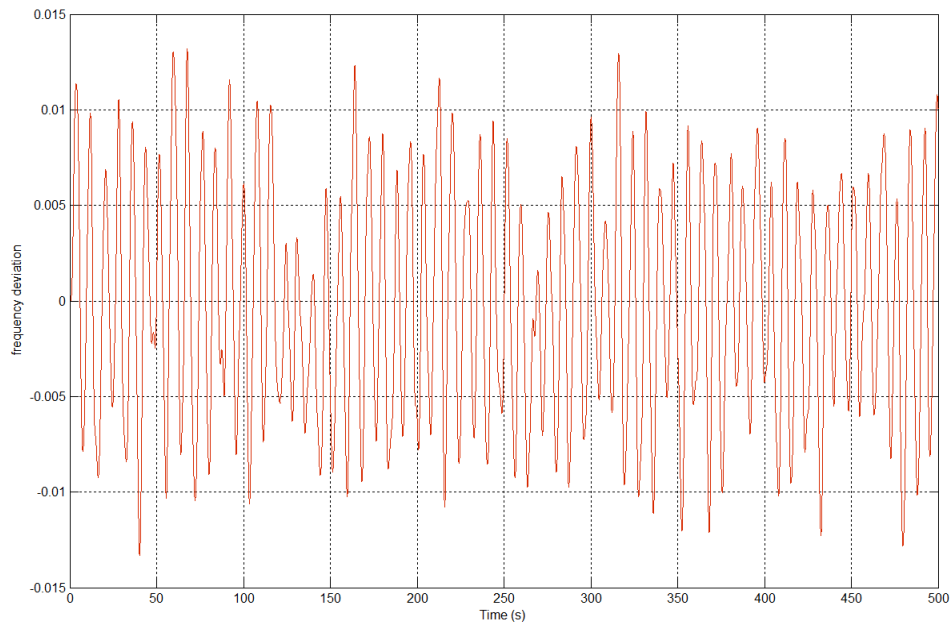


**Figure 12 (b):** Frequency deviation of PID with 10% model uncertainty and measurement noise.

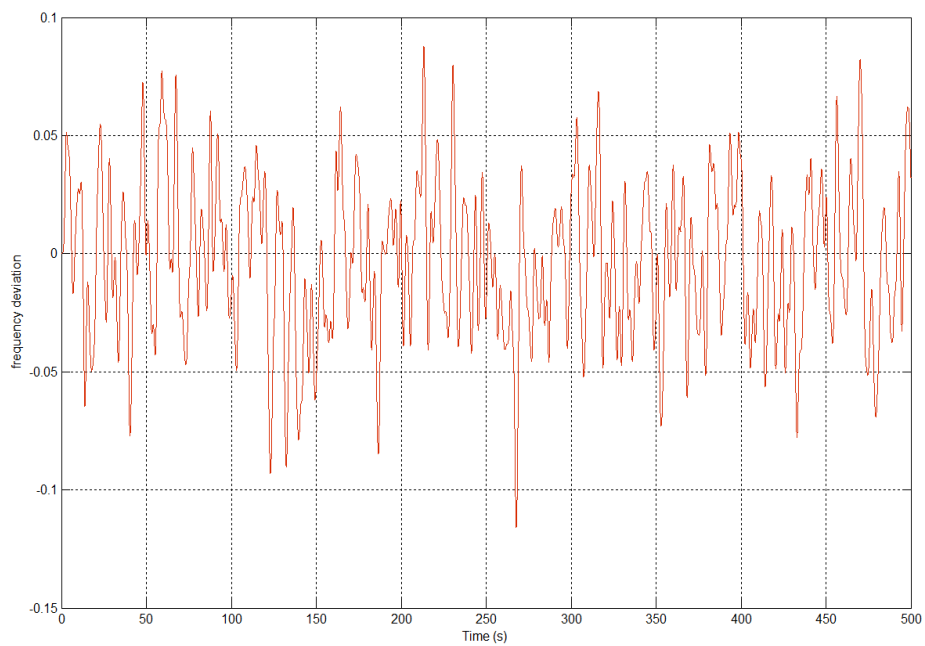


**Figure 13 (a):** Frequency deviations with reduced weights on battery control signal.

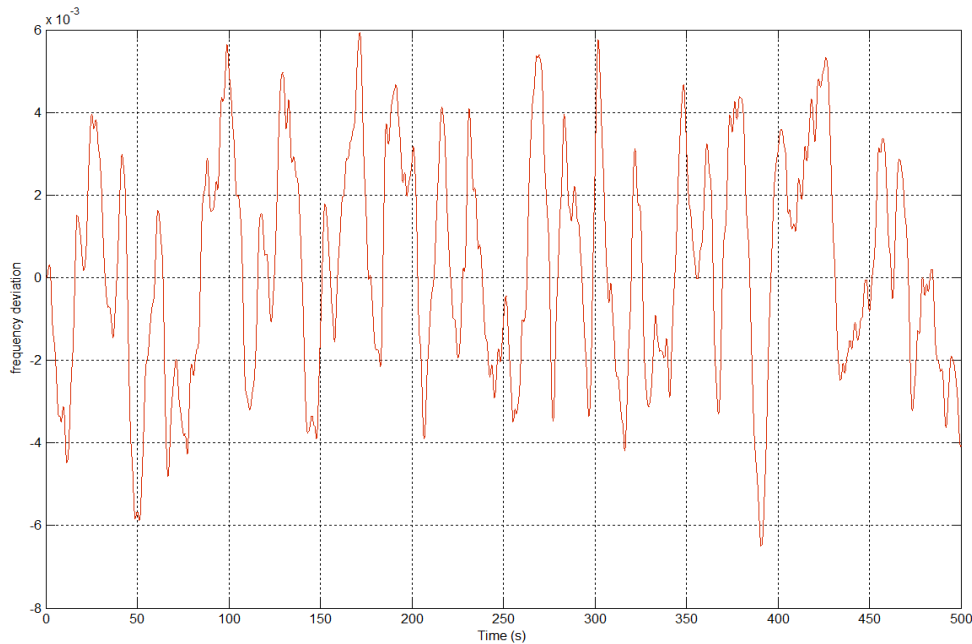


**Figure 13 (b):** Frequency deviations with original weights on battery control signal.

By comparing Figs. 10 and 11, one can see that the latter has more high frequency harmonics on the generator power variation (in green). The reason is that, in this case, there is no battery, and so the generator is forced to compensate the high frequency load/wind power variations. In the former case (Fig. 10), the high frequency components in the system are being smoothed by the battery.

In order to specifically examine system robustness, Fig. 12 shows the system frequency deviation when 10% model uncertainty is added to the diesel engine and rotating mass models, and 10% noise is added to all measurements. Fig. 13 our  $\mu$  synthesis controller design was the result of a careful weight selection process, to achieve the desired robust performance.

## V. CONCLUSION

This paper has presented the microgrid frequency deviation problems caused by load disturbances and renewable energy resources. The objective of this work is to study the performance of robust control of microgrid frequency deviation with an attached storage system and to improve the real power and frequency. The investigation is made on by comparing system frequency deviation between the proposed system (designed via synthesis) and the reference system. This new approach is much more robust, and has better performance, as compared to conventional PID control by using resonant model. In future work, we plan to extend the application of these tools to control of reactive power and voltage in microgrids.

**REFERENCES**

- [1] *The Smart Grid: An Introduction*, U.S. Department of Energy, 2008 [Online]. Available:<http://www.oe.energy.gov/SmartGridIntroduction.htm>
- [2] C. Hernandez-Aramburo, T. Green, and N. Mugniot, "Fuel consumption minimization of a microgrid," *IEEE Trans. Ind. Appl.*, vol. 41, pp. 673–681, May-Jun. 2005.
- [3] T. Goya, E. Omine, Y. Kinjyo, T. Senjyu, A. Yona, N. Urasaki, and T. Funabashi, "Frequency control in isolated island by using parallel operated battery systems applying h-inf; control theory based on droop characteristics," *IET Renewable Power Generat.*, vol. 5, pp. 160–166, Mar. 2011.
- [4] A. M. Howlader, Y. Izumi, A. Uehara, N. Urasaki, T. Senjyu, A. Yona, and A. Y. Saber, "A minimal order observer based frequency control strategy for an integrated wind-battery-diesel power system," *Energy*, vol. 46, no. 1, pp. 168–178, 2012.
- [5] B. Dong, Y. Li, and Z. Zheng, "Control strategies of dc-bus voltage in islanded operation of microgrid," in *Proc. 4th Int. Conf. Electric Utility Deregulat. Restructuring and Power Technolog. (DRPT), 2011*, Jul. 2011, pp. 1671–1674.
- [6] V. Sundaram and T. Jayabarathi, "Load frequency control using PID tuned ANN controller in power system," in *Proc. 1st Int. Conf. Electrical Energy Syst. (ICEES)*, Jan. 2011, pp. 269–274.
- [7] V. P. Singh, S. R. Mohanty, N. Kishor, and P. K. Ray, "Robust h-infinity load frequency control in hybrid distributed generation system," *Int. J. Electr. Power Energy Syst.*, vol. 46, pp. 294–305, 2013.
- [8] R. Dhanalakshmi and S. Palaniswami, "Application of multi stage fuzzy logic control for load frequency control of an isolated wind diesel hybrid power system," in *Proc. Int. Conf. Green Technol. Environmental Conservat. (GTEC)*, Dec. 2011, pp. 309–315.
- [9] F. Dupont, A. Peres, and S. Oliveira, "Fuzzy control of a three-phase step-up dc-dc converter with a three-phase high frequency transformer," in *Proc. Brazilian Power Electron. Conf., COBEP '09.*, Oct. 27–1, 2009, pp. 725–732.